ISSN 1063-7842, Technical Physics, 2017, Vol. 62, No. 4, pp. 547–552. © Pleiades Publishing, Ltd., 2017.
Original Russian Text © N.V. Mikhailova, G.A. Volkov, Yu.I. Meshcheryakov, Yu.V. Petrov, A.A. Utkin, 2017, published in Zhurnal Tekhnicheskoi Fiziki, 2017, Vol. 87, No. 4, pp. 527–532.

SOLID STATE

Failure-Delay Effect in Destruction of Steel Samples under Spalling Conditions

N. V. Mikhailova[a], G. A. Volkov[a,b]*, Yu. I. Meshcheryakov[b], Yu. V. Petrov[a,b], and A. A. Utkin[a,b]

[a] *St. Petersburg State University, Peterhof, St. Petersburg, 198504 Russia*
[b] *Institute of Problems of Mechanical Engineering, Russian Academy of Sciences, St. Petersburg, 199178 Russia*
**e-mail: volkovgrig@mail.ru; yp@YP1004.spb.edu*

Received June 15, 2016

Abstract—Dynamic spalling tests have been run on two batches of 30KhN4M steel samples. Experimental data have been processed with the classical technique based on solution of the elastic wave equation. Three samples have been revealed that demonstrated the failure-delay effect under testing. The incubation-time criterion has been used to show the conditions of emergence of failure delay with the example of triangular loading pulses. A rate strength curve has been constructed for the other samples. It has been shown that the limiting strengths under dynamic loads considerably differ for samples from different batches despite the same chemical composition and static strength.

DOI: 10.1134/S106378421704017X

INTRODUCTION

Spalling failure is one of the main techniques for studying processes that occur in solids in dynamic tension [1–5]. Consideration of wave processes that are typical of the spalling problem makes it possible to determine a stress momentum that leads to failure [1, 2]. As a rule, the so-called acoustic approximation, in which only elastic stresses that act in the spalling zone are taken into account, is used to estimate the spalling momentum parameters.

Sample failure may occur sometime after the maximum of tensile stress has been reached in the spalling section. This implies that the failure moment falls onto the descending or constant segment of effective local stress. This phenomenon was coined as "failure delay," and pulses that correspond to this failure type are, as a rule, close to threshold ones. Threshold pulses are understood to be pulses of given duration and shape that have the minimum failure-producing amplitude. Failure delay has been registered in some spalling experiments, for example, in [6, 7]. However, any detailed discussion of this phenomenon is practically absent from the literature. In a situation like this, strength is often linked, purely formally, to the period of action of tensile stresses in the spalling section [6].

In this article, spalling failure delay is explained using the criterion of an incubation time. The notion of the structural–temporal criterion is based on the following two material characteristics: quasistatic material strength and failure incubation time. These quantities are strength-related parameters of a material; they are independent of experimental conditions and can be applied to different types of loading. This approach proved its effectiveness when determining conditions of emergence of various transients such as brittle fracture [8, 9], electrical breakdown [10], and cavitation in fluids [11].

ONE-DIMENSIONAL WAVE PROBLEM

Spalling failure occurs as follows. A shock pulse creates a compression wave in a sample. The wave propagates along the sample axis until it reaches a free surface. Upon reflection from the surface, the compression wave reverses sign and propagates backwards as a tensile wave. Since the tensile strength of a material is usually considerably lower than its compressive strength, a failure may occur in a certain sample section. Under threshold loads, the failure may reveal itself as microcrack nucleation. With more intense actions, the fraction of the material is completely separated from the sample in the form of the so-called spalling plate.

Solving the one-dimensional spalling problem in its elastic formulation shows that the time profile of the wave of compressive stresses coincides, bar a multiplier, with $V(t)$, the velocity of motion of particles on the free surface. Thus, the time dependence of stresses in the spalling section with a coordinate x can be rep-

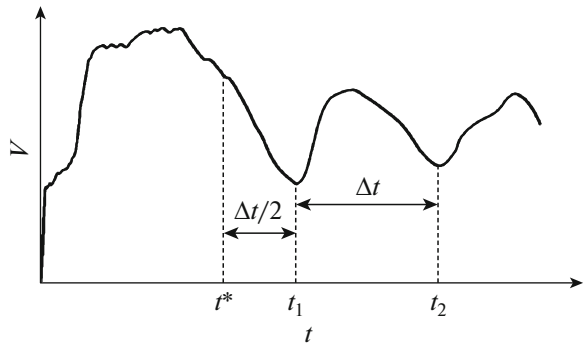

Fig. 1. Dependence of free-surface speed on time.

resented by the sum of compressive and tensile waves as

$$\sigma(x,t)=\sigma^{\text{inc}}+\sigma^{\text{ref}}=\frac{1}{2}\rho a V\left(t-\frac{x}{a}\right)-\frac{1}{2}\rho a V\left(t+\frac{x}{a}\right), \quad (1)$$

where ρ is the material density and a is the propagation speed of a longitudinal stress wave. It should be noted that the temporal profiles of the compressive and tensile waves coincide completely, with the tensile wave lagged behind by $\Delta t = 2x/a$, which is the doubled travel time of the elastic wave through the spalling section.

With the substitution $t' \to t - x/a$, the time dependence in the cross section x^* can be written in the form

$$\sigma(x^*,t') = \frac{1}{2}\rho a\left[V(t') - V\left(t' - \frac{2x^*}{a}\right)\right]$$
$$= \frac{1}{2}\rho a(V_1 - V_2) = \frac{1}{2}\rho a\Delta V.$$

In other words, the stress history in the spalling cross section prior to the failure can be represented as a quantity proportional to the difference between the function of the free-surface speed profile and the same profile shifted by the doubled travel time of the wave across the thickness of the spalling layer [1].

As a rule, the speed $V(t)$ of the sample free surface is measured by interferometry. The coordinate x of the spalling section can be calculated from the spalling pulse duration that coincides with the time Δt (Fig. 1) or simply by measuring the thickness of the spalling plate. At the time moment t_1, the signal about a failure that occurred in the sample reaches the free surface. Accordingly, the time of the very moment of failure equals $t^* = t_1 - \Delta t/2$.

Table 1.

Sample no.	V_0, m/s	σ_{max}, MPa	σ^*, MPa	T_z, ns
19	350	3886	3700	100
22	365	4433	4204	40
25	365	3398	3340	41

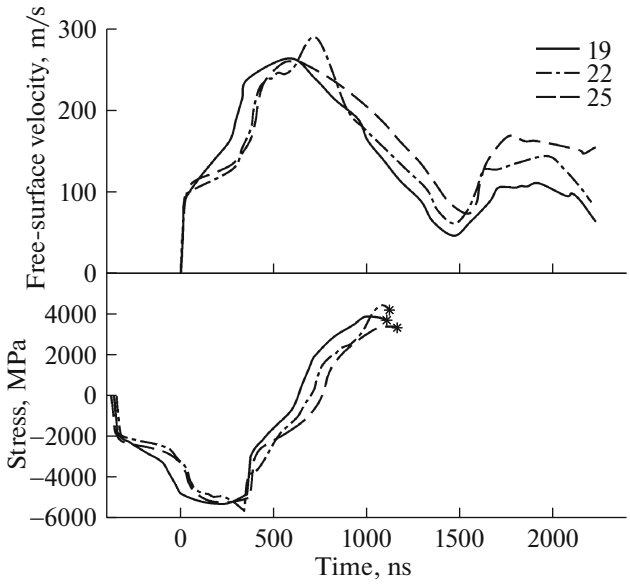

Fig. 2. Time dependences of free-surface speed (top) and stress in the spalling section (bottom) for threshold loadings.

ANALYZING THE RESULTS OF PROCESSING EXPERIMENTAL DATA: FAILURE-DELAY EFFECT

The experiments on spalling failure were carried out under the conditions of the so-called uniaxial deformation, in which the only nonzero component of the deformation tensor is the component that coincides with the direction of wave propagation. Two batches of the 30KhN4M steel samples manufactured under different conditions of thermomechanical treatment were tested. An analysis of the data was performed according to the above solution of the wave problem (1) in which the stress profile in the spalling section is constructed with a shift by the time $\Delta t/2$.

In the case of threshold loads, failure may occur with a delay sometime after the maximum stresses have been reached in the spalling section (Fig. 2). In our experiments, the failure-delay effect was observed for sample nos. 19, 22, and 25 (Table 1). Given the striker speed of 350 m/s and the sample thickness of 1.831 mm, the maximum tensile-stress value could be as high as 3886 MPa. However, it follows from the experimental data that the sample fails under a stress of 3700 MPa, with the failure delay time comprising a value of 100 ns.

INCUBATION-TIME CRITERION

Application of the incubation-time criterion makes it possible to describe many effects that are observed under dynamic testing [8–15]. For example, the phenomenon of failure delay is in close accordance with the main idea of the spatial–temporal approach,

according to which the onset of a failure at a given scale level is necessarily preceded by a preparatory process in which flaws develop with certain characteristic times in the material structure. Therefore, the failure in the spalling section is determined not by the instantaneous values of tensile stresses but by a combination of amplitude and temporal characteristics of the local field of force. For materials free of macroscopic defects, the incubation-time criterion has the form (see, e.g., [14])

$$\int_{t-\tau}^{t} \sigma(s,x)ds < \sigma_c\tau, \qquad (2)$$

where $\sigma(s, x)$ is the stress history in the section x and σ_c is the static material strength while τ is the incubation (structural) time of failure. Thus, for a failure to occur in a given cross section, a momentum of no less than $\sigma_c\tau$ needs to be accumulated. The parameters σ_c and τ are material specific and do not depend on the geometry of the test sample or on the shape or duration of action. Thus, we can say that the static strength σ_c and the incubation time τ form a system of parameters that govern the failure process.

Experimental time dependences of the free-surface speed allow one to reconstruct completely the stress profile in the spalling section up to the failure moment t^*. The incubation time value τ in every particular test can be determined by the immediate substitution of calculated stresses into the criterion in Eq. (2). Calculation results are compiled in Table 2.

Processing post-threshold testing data showed that stresses at the stage of sample tension can be approximately described by the linear dependence

$$\sigma(t) = \dot{\sigma}tH(t). \qquad (3)$$

After substituting a load of the linear form in Eq. (3) into the criterion in Eq. (2) and subsequent integration, we can derive the following simple expression for calculating the incubation time:

$$\tau = 2\left(t^* - \frac{\sigma_c}{\dot{\sigma}}\right). \qquad (4)$$

The calculation of the incubation time by the formula in Eq. (4) produced results comparable to the earlier calculations, thereby confirming the assumption about linear growth of tensile stresses in the tests. Therefore, in order to determine some average integral failure incubation-time value, strength curves $\sigma(\dot{\sigma})$ that correspond to different τ were constructed. Then, the method of least squares was used to determine the curve that most closely matches the experimental points, with the value of τ for this curve being taken as the failure incubation time for the test material. As a result, two values of the incubation time were obtained for each batch of steel, i.e., $\tau_1 = 204$ ns and $\tau_2 = 442$ ns (Fig. 3). It turned out that the samples from one of the batches have a greater dynamic strength with the same static strength of $\sigma_c = 1300$ MPa.

Table 2.

First batch of samples ($\tau_1 = 204$ ns)			Second batch of samples ($\tau_2 = 442$ ns)		
τ, ns	$\dot{\sigma} \times 10^{10}$, MPa/s	σ^*, MPa	τ, ns	$\dot{\sigma} \times 10^{10}$, MPa/s	σ^*, MPa
232	1.95	3355	598	0.778	3710
301	1.62	3432	195	2.580	3630
401	1.19	3322	566	1.200	4470
188	2.83	3563	477	1.320	4507
174	3.18	3555	561	0.958	3926
169	3.55	3791	508	0.963	3734
169	2.73	3397	567	1.140	4336
			597	1.160	4541
			576	0.924	3463
			406	1.320	3650

WAVE RE-REFLECTION PHENOMENON. REALIZATION OF THE FAILURE-DELAY EFFECT

Using the structural–temporal approach makes it possible to determine conditions under which failure occurs with a delay. According to the incubation-time criterion, increase of the amplitude and duration of the threshold pulse leads to a failure. This makes the process of the dynamic failure radically different from a slow quasistatic one where the material cannot be loaded above its static strength σ_c. Therefore, when dealing with shock loading, it seems reasonable to

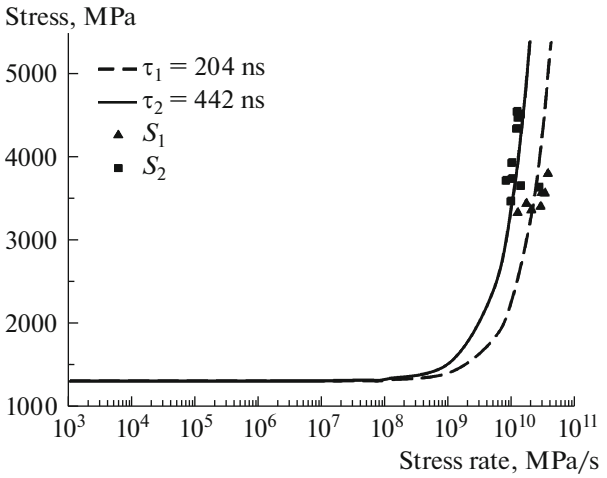

Fig. 3. Rate dependence of limiting stresses obtained for $\tau_1 = 204$ ns and $\tau_2 = 442$ ns and dependence $\sigma(\dot{\sigma})$ for the experimental points. The static strength $\sigma_c = 1300$ MPa.

determine the threshold loads in the form of pulses of a certain shape with fixed amplitude and duration. This entails running a whole series of tests in which the minimum amplitude required for a failure is determined for a given load duration and shape. These experiments were carried out in [15], where the deferred onset of macroscopic-crack formation was observed on the descending branch of the local field of force, i.e., the failure moment was sometime after the intensity coefficient had passed its maximum value.

The most visual way to demonstrate the emergence of the failure-delay effect is to consider triangular loading pulses. Let P be the amplitude of a load pulse and $T = T_1 + T_2$ be its duration, where T_1 and T_2 are the durations of the pulse ascending and descending parts, accordingly. If it is a threshold pulse, failure always occurs on the descending segment of the load pulse, that is, a failure delay is observed. It follows from the criterion in Eq. (2) that the amplitude of this pulse

$$P_{\text{th}} = \begin{cases} \dfrac{2\sigma_c\tau}{T}, & T < \tau, \\ \dfrac{2\sigma_c T}{2T - \tau}, & T > \tau. \end{cases}$$

The following expression holds true for the failure delay time T_d:

$$T_d = \begin{cases} T_2, & T < \tau, \\ \dfrac{T_2\tau}{T}, & T > \tau. \end{cases}$$

Increasing the amplitude of a pulse with fixed rise and fall durations T_1 and T_2 makes the pulse post-threshold. The ratio of the amplitude of a post-threshold pulse to that of the minimum destructive one characterizes the degree of overload. For post-threshold pulses with durations shorter than the incubation time τ, amplitude increase reduces the delay time. If the segment of the load rise is shorter than the fall segment, a failure delay will be observed for any overload. Otherwise, the delay time will decrease to zero, and the amplitude when it becomes zero is determined by the expression $P = 2\sigma_c\tau/(T_1 - T_2)$. Further amplitude increase leads to a situation where the failure condition is simultaneously fulfilled in two sections. One section corresponds to the load rise segment, while in the other section, the stress is decreasing at the failure time moment. The magnitudes of stresses in both sections are the same.

Two scenarios are possible for pulses with durations that exceed the incubation time τ or for pulses with load rise segments shorter that the fall segments, $T_1 < T_2$. In the first scenario, similar to the action of short pulses, failure occurs on the load decay segment. In the second scenario, the failure moment is preceded by a period when the stresses do not change. Such a situation was observed experimentally in [1]. The duration of the stress-constancy period can also be treated as a failure delay, as the stresses remain unchanged and one cannot speak of a rate dependence of strength. Finally, if the loading segment is longer than the load decay segment, $T_1 > T_2$, and the overload is small, failure occurs with a delay, i.e., within the load decay segment. When the overload grows, failure takes place during the rise in the stress level and no failure delay is observed.

Figure 4 presents the normalized stresses in the spalling section depending on the normalized time in different situations, viz., (a) $T < \tau$, $T_1 < T_2$; (b) $T < \tau$, $T_1 > T_2$; (c) $T > \tau$, $T_1 < T_2$; (d) $T > \tau$, $T_1 > T_2$. There are two failure sections in Fig. 4b (dashed line with the larger coordinate), while in Fig. 4c, the dashed-dot, dashed, and solid lines show the incident, reflected, and total stresses. The circle indicates the failure moment.

Thus, no failure delay only occurs when loading with pulses in which the load rise segment is longer than the load fall segment or under big overloads. With arbitrary loading actions, the overall picture that is similar to the one observed with the above pulses in the ideal shape persists. There is a minimum threshold amplitude at which a failure delay occurs for any arbitrarily shaped pulse. Increasing the pulse amplitude will shorten the delay time. Hence, the moment of failure counted from the beginning of the applied pulse takes place sooner. If the applied pulse is non-monotonic, the moment of failure may move further as the amplitude increases. The emergence of conditions under which the failure condition is simultaneously fulfilled in several sections is also possible.

An analysis of the results shows that the condition for the realization of the failure-delay effect depends not only on the amplitude of a shock pulse, but also on its duration. The wave re-reflection phenomenon can emerge in thin samples loaded with prolonged actions. The leading edge of the tensile wave reflects from the surface being loaded and returns to the spalling section to subject it this time to compressive stresses. Then, this wave will again be reflected upon reaching the free surface. Thus, the stress at a point with the coordinate x will have the form

$$\sigma(x,t) = \frac{1}{2}\rho a\left[-V\left(t + \frac{x}{a}\right) + V\left(t - \frac{x}{a}\right) - V\left(t + \frac{x}{a} - \frac{2l}{a}\right) + V\left(t - \frac{x}{a} - \frac{2l}{a}\right) - \ldots\right].$$

Here, l is the sample length and $T_0 = 2l/a$ is the time in which the wave returns to its initial position in the sample. When the argument of the next subsequent term in the sum becomes less than zero, the series can be truncated, since no load is applied at the time moment $t = 0$. The summation of the elastic stresses of unlike signs reduces the intensity of tensile action on the sample. Thus, the overall tensile pulse will not bring about a sample failure. Further increas-

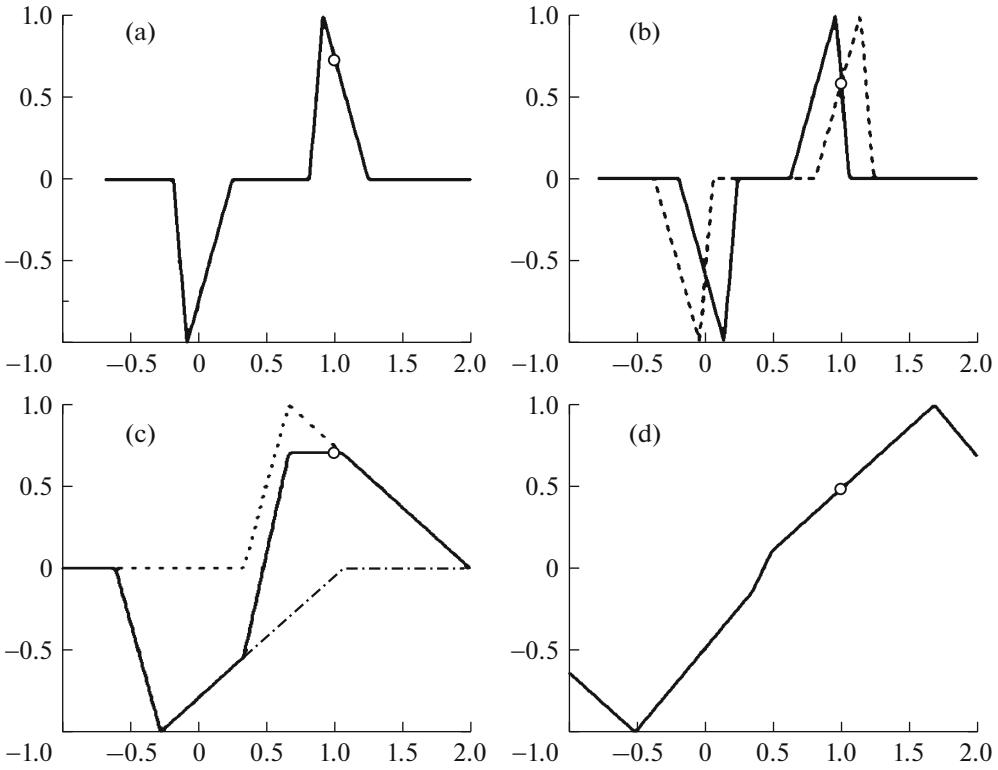

Fig. 4. Stresses in spalling section for different ratios between durations of load rise and fall segments.

ing the striker speed without thickening the sample will lead to post-threshold loads for which the failure-delay effect is not feasible. Therefore, one must precisely balance the duration of action and the sample thickness so as to avoid the re-reflection of the tensile wave.

CONCLUSIONS

An analysis of the experimental data on spalling failure has allowed us to reveal several tests in which the failure delay phenomenon was observed. This effect can be explained by the structural–temporal criterion that also makes it possible to calculate threshold stresses for different loading rates. The strength parameters of the tested material have been determined using the incubation-time criterion. It has been shown that the method of treatment of steel may significantly affect its dynamic strength. The study has enabled us to draw a conclusion that, in order to observe the failure-delay effect, all experimental conditions must be precisely controlled and certain balance must be kept between parameters like the duration and amplitude of action and the sample thickness.

Based on the above results, the following can be concluded. In order to study the strength properties of a material, it should preferably be subjected not only to high-rate overloaded pulses with a high density of supplied energy, but also to threshold actions. In this case, temporal effects that are only typical of the dynamic failure mode can be observed. If loading is performed by high-intensity post-threshold actions, the material will have no time to manifest certain characteristic structural–temporal failure effects due to the high rate of load growth.

ACKNOWLEDGMENTS

This work was supported by the Russian Foundation for Basic Research, projects nos. 17-01-00618, 16-51-53077, and 16-01-00638, as well as the grant of the President of the Russian Federation, project no. MK-7596.2015.1.

REFERENCES

1. N. A. Zlatin, G. S. Pugachev, S. M. Mochalov, and A. M. Bragov, Sov. Phys. Solid State **17**, 1730 (1975).
2. K. B. Broberg, *Cracks and Fracture* (Academic, London, 1999).
3. D. Batani, V. I. Vovchenko, A. V. Kil'pio, I. K. Krasyuk, I. V. Lomonosov, P. P. Pashinin, A. Yu. Semenov, V. E. Fortov, and E. V. Shashkov, Dokl Phys. **48** (3), 123 (2003).
4. Liqiang Lin and Xiaowei Zeng, Eng. Fract. Mech. **142**, 50 (2015).
5. D. A. Dalton, et al., J. Appl. Phys. **104**, 013526 (2008).

6. N. A. Zlatin, G. S. Pugachev, et al., Sov. Phys. Solid State **16**, 1137 (1974).
7. N. A. Zlatin, N. N. Peschanskaya, and G. S. Pugachev, Zh. Tekh. Fiz. **56** (2), 403 (1986).
8. Y. V. Petrov, in *Rock Dynamics and Applications — State of the Art*, Ed. by J. Zhao and J. Li (Taylor, London, 2013), p. 101.
9. V. A. Bratov, A. A. Gruzdkov, S. I. Krivosheev, and Y. V. Petrov, Phys. Dokl. **49**, 338 (2004).
10. Yu. V. Petrov, Phys. Dokl. **59**, 56 (2014).
11. A. A. Gruzdkov, G. A. Volkov, and Yu. V. Petrov, Acoust. Phys. **53**, 119 (2007).
12. Y. V. Petrov and A. A. Utkin, Sov. Mater. Sci. **25** (2), 153 (1989).
13. N. F. Morozov, Yu. V. Petrov, and A. A. Utkin, Sov. Dokl. Phys. **35**, 646 (1990).
14. Yu. V. Petrov, I. V. Smirnov, and A. A. Utkin, Mech. Solids **45**, 476 (2010).
15. A. N. Berezkin, S. I. Krivosheev, Y. V. Petrov, and A. A. Utkin, Dokl. Phys. **45**, 617 (2000).

Translated by V. Potapchouck